Cellular/Molecular

Novel Subcellular Distribution Pattern of A-Type K^+ Channels on Neuronal Surface

Mihaly Kollo, Noémi B. Holderith, and Zoltan Nusser
Laboratory of Cellular Neurophysiology, Institute of Experimental Medicine, Hungarian Academy of Sciences, 1083 Budapest, Hungary

Potassium channels comprise the most diverse family of ion channels. In nerve cells, their critical roles in synaptic integration and output generation have been demonstrated. Here, we provide evidence for a distribution that predicts a novel role of K^+ channels in the CNS. Our experiments revealed a highly selective clustering of the Kv4.3 A-type K^+ channel subunits at specialized junctions between climbing fibers and cerebellar GABAergic interneurons. High-resolution ultrastructural and immunohistochemical experiments demonstrated that these junctions are distinct from known chemical and electrical (gap junctions) synapses and also from puncta adherentia. Each cerebellar interneuron contains many such K^+ channel-rich specializations, which seem to be distributed throughout the somatodendritic surface. We also show that such K^+ channel-rich specializations are not only present in the cerebellum but are widespread in the rat CNS. For example, mitral cells of the main olfactory bulb establish Kv4.2 subunit-positive specializations with each other. At these specializations, both apposing membranes have a high density of K^+ channels, indicating bidirectional signaling. Similar specializations with pronounced coclustering of the Kv4.2 and 4.3 subunits were observed between nerve cells in the medial nucleus of the habenula. Based on our results and on the known properties of A-type K^+ channels, we propose that strategically clustered K^+ channels at unique membrane specializations could mediate a novel type of communication between nerve cells.

Key words: **voltage-gated K channels; immunohistochemistry; cerebellum; hippocampus; olfactory bulb; interneuron**

Introduction

Potassium channels play a key role in many neural functions, including the generation and shaping of action potentials (APs), the regulation of the frequency and the temporal pattern of AP firing during repetitive activation, the modulation of the extent of AP backpropagation in dendrites, the control of the magnitude of synaptic potentials and their integration in dendrites, and setting of the resting membrane potential (for review, see Hille, 2001; Migliore and Shepherd, 2002; Johnston et al., 2003). This functional diversity is paralleled by an enormous molecular heterogeneity (Chandy, 1991; Hille, 2001; Gutman et al., 2003). Potassium channels with widely different molecular structures have been classified based on the number of transmembrane (TM) domains (2, 4, 6, 7, and 8 TM). The six TM family includes voltage-activated and some Ca^{2+}-activated K^+ channels. Genes encoding voltage-gated K^+ channel subunits are members of the Kv family, which consists of >35 subunits in 12 subfamilies (Kv1–12) (Chandy, 1991; Gutman et al., 2003). Members of the Kv subfamilies have closely related primary structures (sequence homology >65%) and similar functional properties. For example, homomeric or heteromeric assemblies of the subunits of the Kv4 subfamily (Kv4.1, Kv4.2, Kv4.3) show rapid activation and inactivation, resulting in transient or A-type K^+ current (I_A).

A-type K^+ channels have received considerable attention and have been investigated extensively using molecular, anatomical, and electrophysiological techniques. For example, dendritic A channels modulate EPSPs and affect EPSP temporal summation in hippocampal CA1 pyramidal cells (PCs) (Hoffman et al., 1997; Cai et al., 2004). Dendritic I_A also reduces the amplitude of the backpropagating action potentials (Hoffman et al., 1997). Because backpropagating APs, when appropriately paired with synaptic inputs, induce long-term modification of EPSPs, mechanisms that modify dendritic I_A will also affect synaptic plasticity (Frick et al., 2004). It has also been demonstrated that the generation and the spread of regenerative Ca^{2+} signals in distal dendrites of PCs are also under the control of dendritic A-type K^+ channels (Cai et al., 2004). These channels are not confined to the somatodendritic domains of nerve cells but may also be present in PC axons where they gate the axonal propagation of APs (Debanne et al., 1997).

Recently, immunohistochemical experiments have been performed to investigate the subcellular distribution of A-type K^+ channel subunits. Light microscopic (LM) immunohistochemistry for the Kv4.2 subunit (the most likely subunit underlying I_A in CA1 PCs) revealed a rather uniform staining of the stratum radiatum (Maletic-Savatic et al., 1995; Varga et al., 2000; Rhodes et al., 2004; Trimmer and Rhodes, 2004; Jinno et al., 2005), despite the convincing functional demonstration that I_A increases in the apical dendrites of CA1 PCs as a function of distance from the

Received Dec. 9, 2005; revised Jan. 17, 2006; accepted Jan. 17, 2006.

Z.N. is the recipient of a Wellcome Trust International Senior Research Fellowship, an International Scholarship from Howard Hughes Medical Institute, European Young Investigator Award, and a Postdoctoral Fellowship from the Boehringer Ingelheim Fond. The financial support from these foundations is gratefully acknowledged. We are grateful to Dr. Ryuichi Shigemoto for the anti-mGluR1α antibody. We thank Drs. Mark Eyre, Mark Farrant, and Istvan Mody for their comments on this manuscript.

Correspondence should be addressed to Zoltan Nusser, Laboratory of Cellular Neurophysiology, Institute of Experimental Medicine, Hungarian Academy of Sciences, Szigony Street 43, 1083 Budapest, Hungary. E-mail: nusser@koki.hu.

DOI:10.1523/JNEUROSCI.5257-05.2006

Copyright © 2006 Society for Neuroscience 0270-6474/06/262684-08$15.00/0

soma (Johnston et al., 1999; Migliore and Shepherd, 2002). Punctuate immunolabeling for the Kv4.2 subunit has also been reported in hippocampal and subicular PCs (Jinno et al., 2005). After electron microscopic (EM) analyses of peroxidase reactions, Jinno et al. (2005) concluded that Kv4.2 subunits are highly enriched in some GABAergic synapses. A similar conclusion was reached by Alonso and Widmer (1997) when they studied the subcellular distribution of the Kv4.2 subunit in the supraoptic nucleus. Here, we examined the subcellular distribution of the Kv4.2 and Kv4.3 subunits using high-resolution immunolocalization techniques to reveal potential nonuniformities in their subcellular distributions. Our results demonstrate a highly uneven distribution of these subunits on the neuronal surface.

Materials and Methods

Wistar rats [postnatal day 14 (P14) to P101] were deeply anesthetized before transcardial perfusion as described previously (Holderith et al., 2003). Sagittal sections (60 μm in thickness) from the cerebellar vermis, horizontal sections from the olfactory bulb, and coronal sections from the forebrain were cut with a vibratome and were washed several times in 0.1 M phosphate buffer. Sections were then blocked in either 10% normal goat serum (NGS) in Tris-buffered saline (TBS) or in 2% bovine serum albumin (BSA) or 10% normal donkey serum (NDS) in TBS (for goat anti-Kv4.3 and Kv4.2 antibodies). After blocking, the sections were incubated in primary antibodies in TBS containing 1–2% NGS, BSA, or NDS and 0.05% Triton X-100. The following primary antibodies were used in the present study: rabbit anti-Kv4.3 (Kv4.3-R, AB5194; 1:500; Chemicon, Temecula, CA), goat anti-Kv4.3 [Kv4.3-G, Kv4.3 (C-17); 1:200; Santa Cruz Biotechnology, Santa Cruz, CA], mouse anti-Kv4.3 (Kv4.3-M, K75/41; 1:500; University of California Davis–National Institute of Neurological Disorders and Stroke–National Institute of Mental Health NeuroMab Facility, Davis, CA), rabbit anti-Kv4.2 (APC-023; 1:500; Alomone Labs, Jerusalem, Israel), goat anti-Kv4.2 [Kv4.2-G, Kv4.2 (C-20); 1:200; Santa Cruz Biotechnology], mouse anti-KChIP1 (K55/7; 1:100; NeuroMab), guinea pig anti-vesicular glutamate transporter 2 (vGluT2) (AB5907; 1:2000; Chemicon), rabbit anti-mGluR1α (AB1551, 1:250, Chemicon; 1:250, one from Dr. Shigemoto, National Institute for Physiological Sciences, Okazaki, Japan), rabbit anti-parvalbumin (PV) (PV-28; 1:1000; Swant, Bellinzona, Switzerland), rabbit anti-calbindin D-28k (CB) (PC-253L, 1:1000; Oncogene, Cambridge, MA), mouse anti-cholecystokinin (CCK) (#9303; 1:1000; CURE/Digestive Diseases Research Center, Antibody/RIA Core, Los Angeles, CA), rabbit anti-neuropeptideY (NPY) (1:15,000) (Csiffary et al., 1990). After several washes, the following secondary antibodies were used to visualize the immunoreactions: biotinylated goat anti-rabbit, goat anti-guinea pig, and donkey anti-goat (Vector Laboratories, Burlingame, CA); Alexa 488 and 594-coupled goat anti-rabbit, goat anti-mouse, goat anti-guinea pig, and donkey anti-goat (Invitrogen, Eugene, OR); 0.8 nm gold-coupled goat anti-rabbit and donkey anti-goat (Aurion, Wageningen, The Netherlands). Ultrasmall gold particles were silver enhanced (EM-SE kit) as described by the manufacturer (Aurion). When the primary antibodies were omitted from the reactions, no specific labeling was observed. The lack of cross reactivity of the secondary antibodies in double-labeling experiments was consistently tested.

Immunofluorescent colocalization of Kv4.3 subunits (Kv4.3-M or Kv4.3-G) and PV, NPY, CB, and CCK was quantitatively analyzed in the CA1 region of the dorsal hippocampus in three rats. For each animal and each double-labeling reaction, 8–14 images (10×) were captured in which the Kv4.3 immunoreactivity of 18–50 neurochemical marker-positive interneurons (INs) was tested. The data are expressed as mean ± SD.

Metabotropic glutamate receptor (mGluR) immunoreactivity was quantified as follows: both antibodies showed qualitatively the same results. Quantifications were done with the anti-mGluR1α antibody obtained from Dr. Shigemoto. Climbing fiber (CF)-IN membrane appositions were systematically searched, photographed, and measured in two animals (81 and 96 μm membrane in 42 and 36 EM images). The part of the somatic and dendritic plasma membrane of the same IN, which was not in contact with CFs, was also measured (196 and 80 μm membrane in 53 and 41 EM images). Gold particles were counted, and if they were within 45 nm from the internal face of the plasma membrane (4 × SD of the Gaussian fit to the radial gold distribution) (Lorincz et al., 2002), they were considered to be associated with the plasma membrane. Nonspecific labeling densities were measured over the nuclei (0.58 and 1.02 particle/μm^2; 1.4 and 2.2% of the specific labeling) and were subtracted from the plasma membrane densities as described previously (Lorincz et al., 2002).

Postembedding immunogold localization of glutamate receptor subunits was performed as described previously (Nusser et al., 1998) with polyclonal rabbit anti-GluR2/3 (AB1506; dilution 1:50–100; Chemicon) and rabbit anti-NR2A/B (AB1548; dilution 1:10; Chemicon) antibodies. Colloidal 10 nm coupled goat anti-rabbit secondary antibodies (British BioCell, Cardiff, UK) were used to visualize the reactions.

For high-resolution morphological investigations, brains were fixed with high glutaraldehyde-containing fixatives (1–2%). All tissues for EM were treated with 0.5–1% OsO_4, 0.5% uranyl acetate, were dehydrated and embedded into Epoxy resin. Digital images were captured with a cooled CCD camera (Cantega; Soft Imaging System, Munster, Germany). All measurements were performed with the aid of Analysis software (Soft Imaging System). Data are given as mean ± SD.

Results

Uneven cell surface distribution of Kv4.3 subunits in cerebellar interneurons

We investigated the cellular distribution of the Kv4.3 subunit in the cerebellar cortex and observed immunopositive GABAergic interneurons (INs, both stellate and basket cells) throughout the molecular layer similar to that found previously (Hsu et al., 2003). Examination of the reactions at high magnifications (Fig. 1) revealed an uneven distribution of the immunoreactive Kv4.3 subunits in these cells. Strongly positive clusters dominated the weaker, homogeneous labeling of the somatodendritic plasma membranes. The size and the location of the clusters greatly varied, some clusters were present at the somatic, and some were present at proximal and distal dendritic locations. Reconstructions of individual neurons demonstrated that single cells contained dozens of clusters (Fig. 1*E*,*F*). To exclude the possibility that the nonhomogeneous distribution of immunoreaction is attributable to cross reactivity of our antibody with another protein, we performed double-labeling experiments with two anti-Kv4.3 antibodies (Kv4.3-R and Kv4.3-G) raised against different, nonoverlapping epitopes in different species (see Materials and Methods). The identical labeling (Fig. 1*A–D*) obtained with the two antibodies demonstrated that both the weak homogenous labeling and the strong clusters were the consequence of specific recognition of the Kv4.3 subunit. We also performed experiments with a third antibody (Kv4.3-M). This monoclonal antibody was raised against a fusion protein that partially overlaps with the epitopes of the two polyclonal antibodies. The immunolabeling pattern obtained with the monoclonal anti-Kv4.3 antibody was also indistinguishable from that obtained with the polyclonal ones.

EM examination of immunogold reactions also revealed an uneven distribution of gold particles along the somatodendritic plasma membranes of INs (Fig. 2). A low density of immunogold labeling was found over the largest part of the plasma membrane, but occasionally strongly immunopositive clusters were also observed. The placement of clusters was not random, but the enrichments were consistently found in regions of the IN plasma membrane that were in direct contact with CFs. CF terminals were identified by their fine structural characteristics (Palay and Chan-Palay, 1974) and also by their immunoreactivity for vGluT2 (Fig. 2*E*,*F*) (Fremeau et al., 2001).

To quantitatively assess the frequency of coassociation of CFs and Kv4.3 subunit-containing clusters, we performed two series of experiments. In double Kv4.3 (immunogold) and vGluT2 (immunoperoxidase) reactions, first we systematically searched for vGluT2-positive CF terminals and assessed in serial sections (60–100 sections) whether they made direct contacts with GABAergic INs. If they made a contact, we evaluated whether the membrane apposition contained Kv4.3 immunogold clusters or not. In two animals, 6 of 8 and 11 of 12 membrane appositions were strongly immunopositive for the Kv4.3 subunit, demonstrating that the majority of the CF-IN membrane appositions contain a high density of Kv4.3 subunit. In the second set of experiments, we assessed the proportion of Kv4.3 clusters that were associated with CFs. In one animal, 10 of 10 clusters were associated with CFs, and in the second animal, only 1 of 10 clusters was contacted by a presynaptic axon of unidentified origin; the remaining axons were positively identified as CFs. Thus, our results demonstrate that almost all (95%) immunogold clusters were apposed to CFs, and the majority (85%) of CF-IN appositions contained high concentrations of A-type K^+ channels.

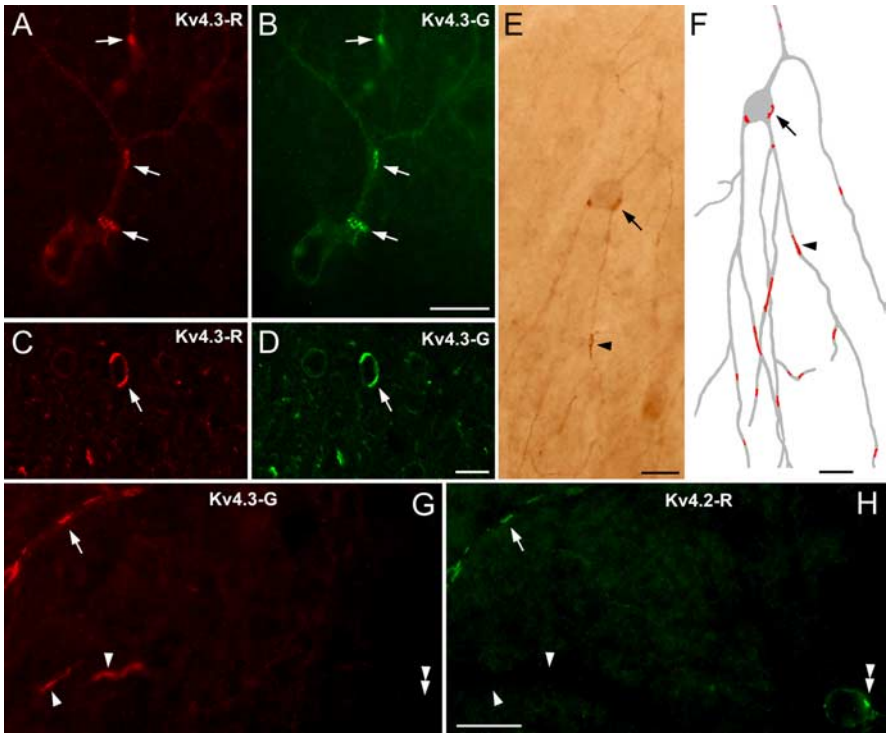

Figure 1. Clustered distribution of A-type potassium channels in the cerebellum. ***A***, ***B***, Light microscopic images of the cerebellar cortex demonstrate the uneven distribution of Kv4.3 subunits in molecular layer INs (clusters indicated by arrows). Identical labeling was obtained with two antibodies against the Kv4.3 subunit (Kv4.3-R, ***A***, ***C***; Kv4.3-G, ***B***, ***D***), indicating the specificity of the immunoreaction. ***C***, ***D***, Prominent clustering of the immunosignal (e.g., arrows) is shown in confocal laser-scanning microscopic images. ***E***, The nonuniform distribution of the Kv4.3 subunit is also observed in peroxidase reactions, a high-sensitivity technique that allows LM reconstruction of immunostained INs. ***F***, The reconstruction illustrates that a single IN (gray) contains several dozens of clusters (red) at somatic (arrow) and dendritic (arrowhead) locations. ***G***, ***H***, Double immunofluorescent labeling for Kv4.3 (***G***) and Kv4.2 (***H***) subunits shows the coclustering (e.g., arrow) of these subunits in some IN dendrites. Several Kv4.3-positive clusters do not contain the Kv4.2 subunit (arrowheads), whereas few Kv4.2 immunopositive clusters (double arrowhead) are immunonegative for Kv4.3. Scale bars, 10 μm.

Interestingly, the part of the IN plasma membrane that was in direct contact with a CF was not homogeneously immunolabeled for the Kv4.3 subunit, but gold particles formed a number of small clusters (Figs. 2*A–D*, 3*A*). This inhomogeneity in the labeling was also apparent at very high magnification LM fluorescent images, where large clusters seemed to be further structured (Figs. 1*A*,*B*, 6*F*,*G*). To have a better idea about the spatial organization of the K^+ channel-rich membrane domains, we reconstructed in three dimensions IN somatic and dendritic plasma membranes, which were contacted by CFs. The three-dimensional (3D) reconstructions confirmed that the entire CF-IN membrane apposition did not contain a high density of immunogold particles (Fig. 3*B*) and revealed a complex mosaic of labeling. Exactly the same phenomenon was observed in a fortunate case when a CF-IN membrane apposition was tangentionally cut (*on face* view), revealing a ring of high-density labeling (Fig. 3*D–G*, full view in serial sections). Because the CF-IN membrane appositions were inhomogeneously labeled by gold particles, we examined whether the K^+ channel-rich domains had different ultrastructural features than the gold particle-lacking membranes. In reactions with optimal ultrastructural preservations, the association of high-density gold particles with unique membrane specializations was apparent (Fig. 2*B*,*C*).

Kv4.3 subunit-rich membrane specializations are distinct from chemical and electrical synapses

To test whether the enrichment of the Kv4.3 subunits is a feature of known chemical or electrical synapses or whether they occupy a novel type of subcellular junction, we compared the molecular content and the ultrastructural features of Kv4.3 subunit-rich membrane specializations to those of chemical synapses and gap junctions. Dissimilarity from gap junctions was apparent from the presence of a widening of the extracellular space between the axonal and dendritic plasma membranes instead of the tight apposition of the membranes that characterizes gap junctions. The following sets of evidence prompted our conclusion that the A-type K^+ channel-rich membrane specializations are also distinct from chemical synapses. Clustering of presynaptic vesicles at the presynaptic active zone is essential for the vesicular release of transmitter at chemical synapses, but we never observed vesicle clusters or docked vesicles at the axonal side of these specializations. Additional evidence that synaptic vesicles do not play a role at these specializations came from the observation that Kv4.3-positive clusters were also present between the vesicle-lacking preterminal axon of CFs and INs (Fig. 2*D*,*F*).

Next, we prepared tissue for optimal ultrastructural preservation to characterize the membrane specializations between CFs and INs at high magnifications (Fig. 4). The specializations appeared symmetrical; no obvious polarization between the axon terminal and the plasma membrane of INs was observed (Fig. 4*A*,*B*). Rigid apposition of axonal and dendritic membranes was clearly visible with some thickening of the membranes. The extracellular space was significantly narrower than the synaptic cleft of neighboring chemical asymmetrical synapses on PC spines (14.1 ± 1.5 vs 21.3 ± 2.5 nm; mean ± SD; $n = 38$ and 8, respec-

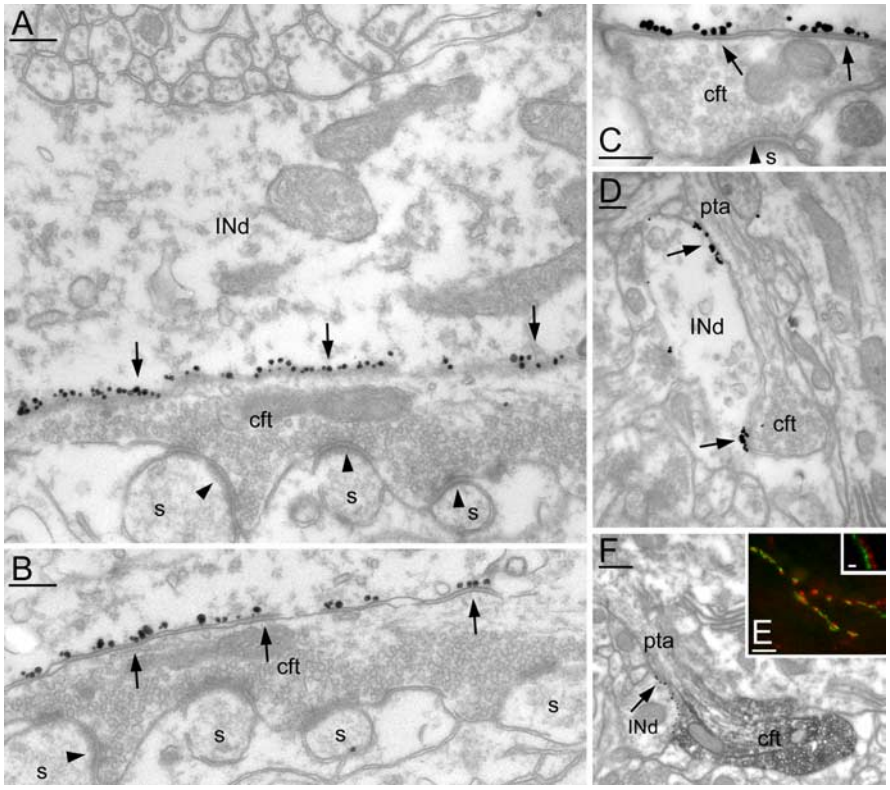

Figure 2. Electron microscopic demonstration of the clustering of the Kv4.3 subunit in specialized junctions. ***A***, ***B***, Part of the dendritic plasma membrane of a cerebellar IN (INd), which is in direct contact with an axon terminal (cft), contains a large number of gold particles (arrows). The axon terminal (cft) establishes three asymmetrical synapses (arrowheads) with PC spines (s) and has ultrastructural features of a CF terminal. The micrograph in ***B*** illustrates the consistency of the labeling in a serial section. By tilting the section in the EM, the rigid appositions between the membranes (arrows) are better seen. ***C***, Higher-magnification view of Kv4.3 immunopositive clusters (arrows) on an IN soma. The CF terminal (cft) establishes an asymmetrical synapse (arrowhead) on a spine (s). ***D***, Nonuniform Kv4.3 immunoreactivity is shown in an IN dendrite (INd). Gold particles are clustered in the dendritic membrane (arrows), where it is in contact with either the CF terminal (cft) or with its preterminal axon (pta). ***E***, Double fluorescent labeling for Kv4.3 (green) and vGluT2 (red) demonstrates that Kv4.3 clusters are apposed to vGluT2 immunopositive CF terminals. The inset shows the lack of full overlap of the green and red spots. ***F***, EM double labeling for Kv4.3 (particles) and vGluT2 (peroxidase reaction), in which the preterminal axon (pta) of a vGluT2-positive CF contacts an IN dendrite (INd) clustering of Kv4.3 (arrow) is detected. Note that the DAB reaction is present in the CF axon terminal (cft) but not in the preterminal axon. Scale bars: ***A–D***, 0.2 μm; ***E***, 15 μm; ***E***, inset, 2 μm; ***F***, 0.4 μm.

tively; $p < 0.001$, unpaired t test). No sign of any postsynaptic density was found at CF-IN specializations, which clearly distinguishes them from both type I synapses and from puncta adherentia. These results are in excellent agreement with a previous study, showing the lack of chemical synapses between CF terminals and molecular layer INs (Hamori and Szentagothai, 1980).

An essential feature of glutamatergic synapses is the presence of postsynaptic GluRs either inside (ionotropic GluRs) or surrounding (metabotropic GluRs) the postsynaptic specializations (Nusser et al., 1994). Because most glutamatergic synapses contain postsynaptic AMPA-type glutamate receptors, first we tested for their presence at CF-IN appositions using postembedding immunogold localizations for GluR2/3 subunits. As shown in Figure 5*A*, despite the concentration of a large number of gold particles in CF to PC spine synapses, no gold particle was found in the CF-IN membrane apposition. Next, we examined the presence of NMDA-type GluRs with an anti-NR2A/B antibody. All examined CF-IN membrane appositions were immunonegative for NR2A/B (Fig. 5*B*), despite the strong immunolabeling of hippocampal Schaffer collateral CA1 pyramidal cell synapses (Fig. 5*C*), which are known to have immunoreactive NMDA receptors. Finally, we also examined the subcellular distribution of the 1α subtype of metabotropic GluRs (mGluR1α), which is the only postsynaptic mGluR expressed by molecular layer INs (Shigemoto and Mizuno, 2000). From our immunogold reactions, it was apparent that the entire IN somatic and dendritic plasma membranes were labeled for mGluR1α, including the parts of the membranes that were contacted by CFs (Fig. 5*D*). To assess whether the CF-IN membrane appositions had a higher density of labeling than the rest of the plasma membrane, we quantified the immunogold reaction in two animals. The density of immunogold particles in CF-IN appositions was 1.8 and 2.0 particle/μm, which were very similar to the densities obtained over the rest of the plasma membrane (1.4 and 2.0 particle/μm), demonstrating the lack of enrichment of mGluR1α in these membrane specializations. Although excluding the presence of all chemical synapse-associated proteins from CF-IN specializations seems an impossible task at present, all of our data indicate that these K^+ channel-rich specializations are distinct from excitatory synapses.

Widespread distribution of A-type K^+ channel-rich junctions in the CNS

Clustered immunoreactivity for the Kv4.3 subunit on the neuronal surface was observed in many brain regions, including the thalamus, hypothalamus, habenula, hippocampal formation, neocortex, and olfactory bulb, indicating that clustered distribution of A-type K^+ channels is not a unique feature of the cerebellar circuit but is widespread in the rat CNS (Fig. 6). For example, a subset of hippocampal GABAergic interneurons was strongly Kv4.3 immunopositive, as described previously (Rhodes et al., 2004), with the somatic and dendritic plasma membranes containing several immunopositive clusters (Fig. 6*A*). EM examination showed in some cases an enrichment of gold particles in membrane specializations (Fig. 6*B*,*C*) similar to those found between cerebellar CFs and INs. However, it is important to note that similar to the cerebellar INs, gold particles labeling Kv4.3 subunits were not exclusively present within these clusters, but a low density of particles was found over the entire somatodendritic plasma membrane. To identify the interneuron subtypes expressing Kv4.3 subunits, we have performed double immunofluorescent labeling for Kv4.3 and PV, CB, CCK, and NPY (supplemental figure, available at www.jneurosci.org as supplemental material). Virtually all NPY (97 ± 3%; $n = 3$), 92 ± 5% of the CCK, 75 ± 5% of the CB, and 50 ± 3% of the PV-positive INs contained the Kv4.3 subunit, demonstrating that the Kv4.3 immunopositive hippocampal INs comprise a diverse population.

In our final series of experiments, we tested whether other subunits of the A-type K^+ channels were also concentrated at these unique membrane specializations. Because the other most abundant A-type K^+ channel subunit is Kv4.2 in the CNS, we performed LM and EM localizations of this subunit in the rat

brain. In the cerebellar cortex, in addition to the strongly positive granule cells, intensely and inhomogeneously labeled INs were observed at the border of the molecular and Purkinje cell layers. As shown in Figure 1, *G* and *H*, some Kv4.3-positive clusters also contained Kv4.2 subunits. An even more prominent colocalization of these two subunits was observed in the medial habenular nucleus. Although the Kv4.2 subunit is present within the whole nucleus and the Kv4.3 subunit is only present in the medial part, in Kv4.3 immunopositive cells, the Kv4.2 subunit has an identical distribution to that of Kv4.3 (Fig. 6*F*,*G*). These cells contained clustered immunoreactivity on the parts of their cell body that were in direct contact with neighboring somata. The discovery of A-type K^+ channel interacting proteins (KChIPs) (An et al., 2000) prompted us to test their presence in these strongly Kv4.2 and Kv4.3 immunopositive clusters. Double immunofluorescent experiments revealed the coclustering of KChiP1 with Kv4.2 and Kv4.3 on the somatic plasma membranes of these cells. EM immunogold analyses revealed a clustered distribution of gold particles for Kv4.2 in the somatic membranes of habenular neurons (Fig. 6*H*). Gold particle clusters were present in both membranes forming the membrane specializations, consistent with the fact that the neuronal elements at both sides of the specializations are identical and express this subunit. Probably the most convincing piece of evidence supporting our conclusion that the K^+ channel-rich membrane specializations are distinct from chemical synapses came from these experiments in the medial habenula. The somata of these cells do not contain the molecular machinery needed for chemical synaptic communication and do not have somatosomatic chemical synapses but contain a large number of K^+ channel-rich specializations.

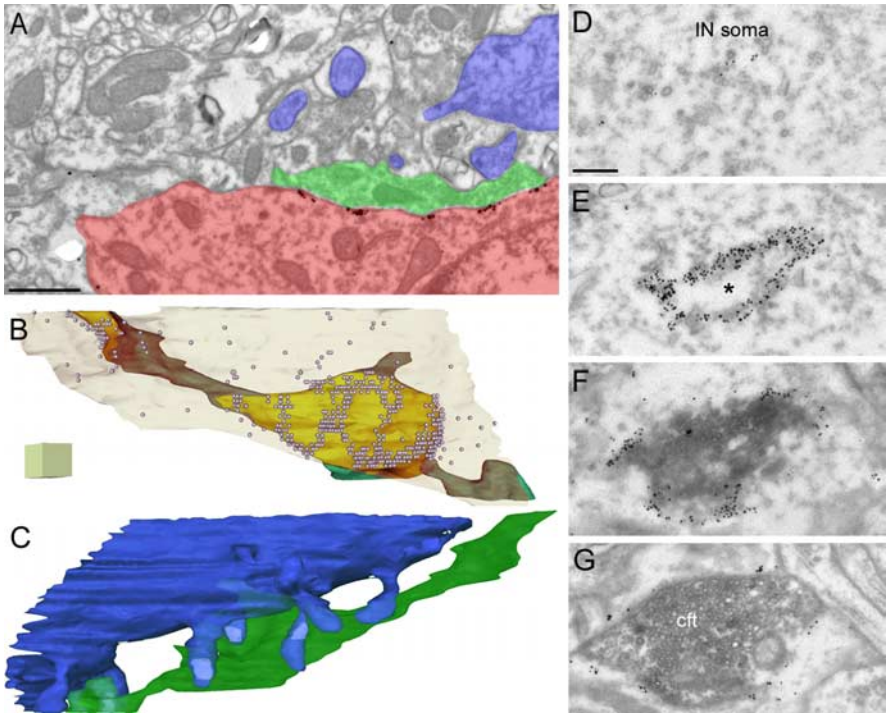

Figure 3. Complex structures of the Kv4.3 subunit immunopositive specializations. ***A***, Electron micrograph of the cerebellar molecular layer showing clusters of Kv4.3 immunogold particles along the somatic plasma membrane of an IN (red). The CF terminal is green, and the PC dendrite and spines are blue. The illustrated micrograph is one of the 44 serial sections on which the 3D reconstruction (shown in ***B*** and ***C***) is based. ***B***, Three-dimensional reconstruction of a CF terminal (green; brown when viewed through the transparent IN membrane) viewed through the transparent IN somatic membrane (light cream). The area of the IN plasma membrane, which is in direct contact with the CF, is yellow. Gold particles are illustrated with small spheres. Note that the high concentration of gold particles does not cover the entire yellow area, but a complex mosaic of K^+ channel-rich domains can be seen. ***C***, The same 3D reconstruction illustrating the Purkinje dendrite and spines (blue) and the CF terminal. Several excitatory synapses (light blue) on PC spines (blue) are established by the CF terminal (green), viewed from the opposite side as in ***B***. ***D–G***, Electron micrographs of consecutive serial sections of an IN, demonstrating the nonhomogeneous labeling of the membrane apposition between a vGluT2-positive CF terminal (peroxidase reaction) and an IN soma. *En face* view of the membrane apposition, showing a strongly immunopositive ring with a negative center (*). Scale bars: ***A***, 0.8 μm; ***B***, ***C***, each side of the cube is 0.5 μm; ***D–G***, 0.2 μm.

Perhaps the most striking example of the uneven distribution of Kv4.2 subunits was observed in the main olfactory bulb. Mitral cell somata and dendrites were decorated by large, intensely labeled clusters (Fig. 6*D*). EM immunogold analyses revealed that the strongly labeled clusters were also located in membrane specializations (Fig. 6*E*), similar to those found in the cerebellum, hippocampus, and habenula. However, similar to the junctions in the medial habenula, both membranes forming the specializations contained a large density of gold particles (Fig. 6*E*). Sometimes, these Kv4.2 subunit-rich specializations between mitral cell dendrites were closely associated with membrane specializations having ultrastructural features of gap junctions, which are widely present between these cells (Schoppa and Westbrook, 2002; Kosaka and Kosaka, 2003).

Discussion

Our high-resolution immunolocalization experiments have demonstrated an uneven distribution of A-type K^+ channel subunits on the surface of nerve cells. These K^+ channels are concentrated in a novel type of membrane specialization and are also present at lower densities in the rest of the plasma membrane. Uneven distributions of some voltage-gated K^+ channel subunits have been reported in the past few years. The first report by Alonso and Widmer (1997) described clustered distribution of Kv4.2 subunit in the somata of nerve cells of the supraoptic nucleus. Using electron microscopy, they found that high-intensity spots of peroxidase reaction end-products were associated with postsynaptic membranes. An almost identical conclusion was reached by Jinno et al. (2005) by studying the subcellular distribution of Kv4.2 subunit in the hippocampus. A postsynaptic enrichment of the Kv4.2 subunit was concluded to underlie the clustered reactivity observed at the LM level. In light of the conclusions of these studies, we have taken utmost care when judging whether Kv4.3 and Kv4.2 subunits were concentrated in chemical synapses or not. We analyzed the K^+ channel-rich membrane specializations at high resolution in tissues prepared for optimal structural preservation and compared them to known type I and type II chemical synapses, puncta adherentia, and gap junctions. Furthermore, because CFs are glutamatergic, we performed a series of GluR localization experiments to test whether the CF-IN membrane specializations showed an enrichment of ionotropic or metabotropic GluRs. All of our experiments prompted us to conclude that these K^+ channel-rich specializations are distinct from known chemical synapses and from gap junctions. It is

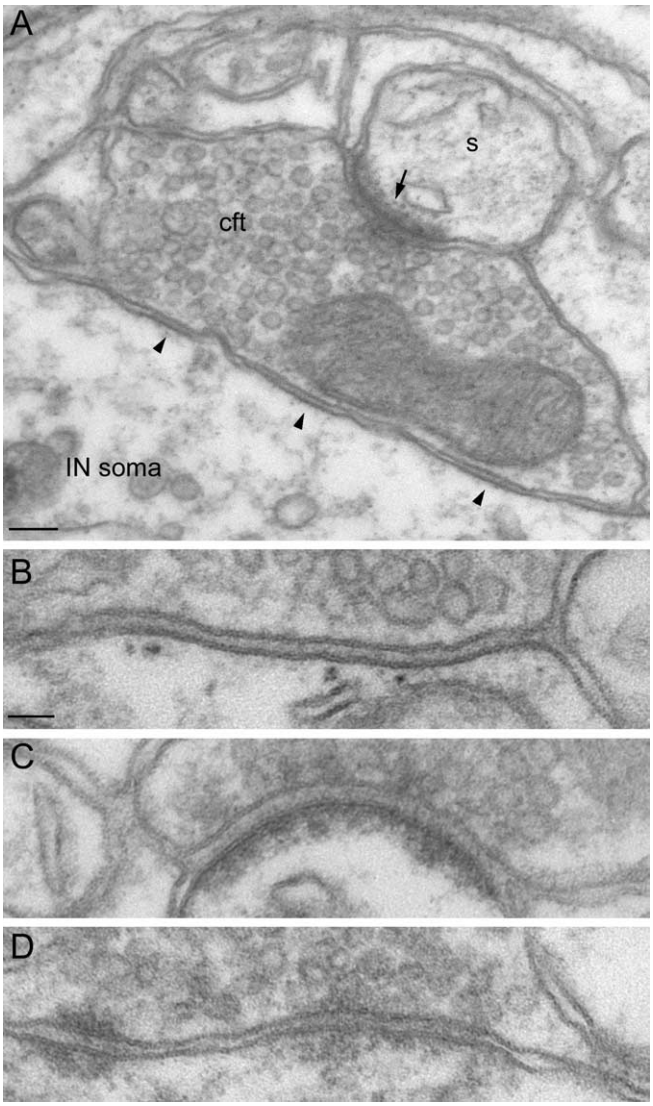

Figure 4. Structural evidence that the Kv4.3 subunit-rich specializations are distinct from known chemical synapses. ***A***, A CF terminal in the cerebellar molecular layer establishes an asymmetrical (type I) chemical synapse (arrow) with a PC spine (s) and several membrane specializations (arrowheads) with an IN soma. ***B–D***, High-magnification views of a membrane specialization between a CF terminal and an IN (***B***), an asymmetrical (type I) chemical synapse made on a Purkinje spine (***C***), a symmetrical (type II) synaptic junction (***D***, right), and a punctum adherens (***D***, left) on an IN dendrite. The presence of presynaptic vesicle clustering distinguishes type I and type II synapses from the CF-IN membrane specializations. Rigid apposition of the presynaptic and postsynaptic membranes characterizes all types of junctions. Scale bars: ***A***, 100 nm; ***B–D***, 50 nm (same magnification).

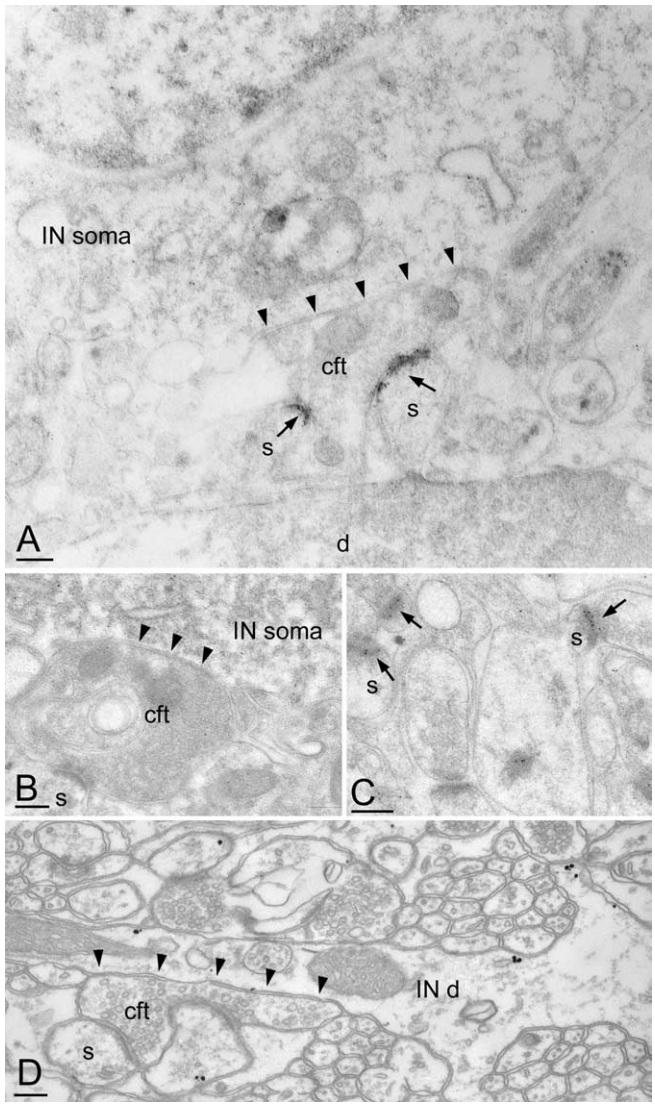

Figure 5. Immunohistochemical demonstration that the membrane specializations between CFs and INs are distinct from glutamatergic synapses. ***A***, Postembedding immunogold localization of the GluR2/3 glutamate receptor subunits in the cerebellar molecular layer. Gold particles are concentrated in the asymmetrical synapses (arrows) made by a CF terminal (cft) with Purkinje cell spines (s), but the membrane apposition between the terminal and the IN somatic plasma membrane (arrowheads) is immunonegative. ***B***, ***C***, Postembedding immunogold localization of the NMDA receptor NR2A/B subunits in the cerebellum (***B***) and in the hippocampus (***C***). The membrane specialization between a CF terminal and an IN soma (***B***, arrowheads) does not contain any gold particle for the NR2A/B subunits, but in the same reactions, Schaffer collateral synapses (***C***, arrows) on hippocampal CA1 pyramidal cell spines (s) are strongly immunopositive. ***D***, Pre-embedding immunogold reaction for mGluR1α in the cerebellar molecular layer. The membrane apposition (arrowheads) between a CF terminal (cft) and an IN dendrite contains gold particles at approximately the same density as in the rest of the IN plasma membrane. Scale bars, 0.2 μm.

apparent from previous studies (Alonso and Widmer, 1997; Muennich and Fyffe, 2004; Jinno et al., 2005) that the high-density of K^+ channel immunoreactivity is present in parts of the somatodendritic plasma membranes that are in direct contact with axon terminals. However, it remains to be determined whether these axosomatic/axodendritic K^+ channel-rich membrane appositions are indeed the sites of chemical synaptic communications, or the situation is similar to our findings at the CF-IN junctions. For example, EM immunogold double-labeling experiments for Kv4.2 and glutamate/GABA receptors could provide an answer to this question.

The functional roles of these A-type K^+ channel-rich membrane specializations are yet unknown. One possibility is that these specializations are the sites of a novel type of interneuronal interaction. Although we have no evidence, we propose a possible functional role of their activation. K^+ channels at these junctions could be activated by changes in membrane potential, resulting in a local and transient alteration in the K^+ conductance of the membrane. As a consequence, membrane depolarization would be followed by a transient hyperpolarization, whereas hyperpolarization by deactivating standing I_A would result in a subsequent depolarization. In both cases, the critical functional consequence of the activation of these junctions is the generation of an alternating response. The initial change in the membrane poten-

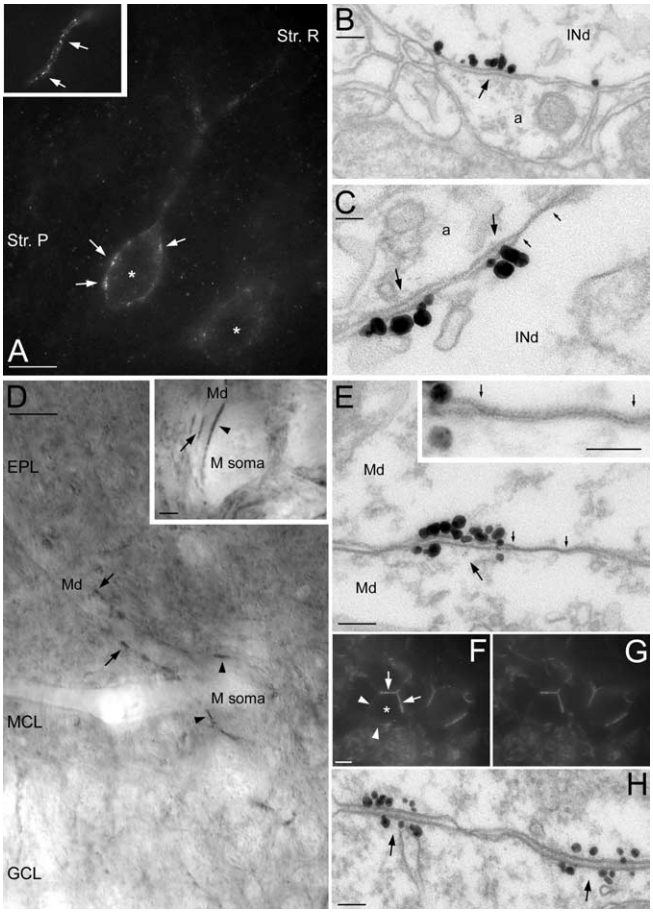

Figure 6. A-type K^+ channel-rich specializations are present throughout the CNS. ***A***, LM immunofluorescent labeling for the Kv4.3 subunit in the hippocampal CA1 area. Kv4.3 immunopositive interneurons (*) are shown with several intensely labeled clusters (arrows) decorating the somatic plasma membrane. The inset illustrates that dendritic immunoreactivity is also highly nonuniform. ***B***, ***C***, EM demonstration of the clustering of gold particles (arrows) for Kv4.3 subunit in hippocampal IN dendrites (INd). A gap junction (marked by small arrows in ***C***) is found next to the K^+ channel-rich specialization. ***D***, Nonuniform distribution of the Kv4.2 subunit in mitral cells of the main olfactory bulb. Several intensely labeled spots are present in the somatic (arrowheads in M soma) and dendritic (arrows in Md) membranes of a mitral cell. The inset shows strongly immunopositive clusters between a mitral cell soma and a dendrite (arrowhead) and between two dendrites (arrow). ***E***, Clustering of gold particles (arrow) between two mitral cell dendrites (Md). A large number of immunogold particles for the Kv4.2 subunits is present at both sides of the specialization. Note the presence of a gap junction (marked by small arrows) next to the gold cluster. The gap junction is illustrated at a higher magnification in the inset. ***F***, ***G***, Double immunofluorescent labeling for Kv4.3 (***F***) and Kv4.2 (***G***) subunits in the medial habenular nucleus. The somata of immunopositive cells (*) are not uniformly labeled, but strongly immunopositive clusters (arrows) are found where cell bodies are in direct contact with each other, whereas the rest of the somatic membrane (arrowheads) is only weakly labeled. ***H***, EM immunogold localization of the Kv4.2 subunit in the medial habenula demonstrates the clustering of particles at both membranes forming the specializations (arrows). Str. P, Stratum pyramidale; Str. R, stratum radiatum; EPL, external plexiform layer; GCL, granule cell layer; MCL, mitral cell layer. Scale bars: ***A***, ***D***, ***F***, ***G***, 10 μm; ***D***, inset, 2 μm; ***B***, ***E***, ***H***, 100 nm; ***C***, ***E***, inset, 50 nm.

tial may be the consequence of an ephaptic interaction between the coupled nerve cells, or it could be mediated either through gap junctions or through conventional chemical synapses. However, a "retrograde" interaction may also be possible. The activity of the INs could be signaled back to CFs through a local elevation of $[K^+]$ in the extracellular space, which may affect the probability of transmitter release from CFs. Finally, it is also conceivable that these K^+ channels may be activated or modulated by intracellular mechanisms, after the nonvesicular release of neurotransmitter substances other than glutamate from CFs. Such neuromodulators, their receptors or target molecules, and the second messengers remain to be identified at CF-IN junctions.

References

Alonso G, Widmer H (1997) Clustering of Kv4.2 potassium channels in postsynaptic membrane of rat supraoptic neurons: an ultrastructural study. Neuroscience 77:617–621.

An WF, Bowlby MR, Betty M, Cao J, Ling HP, Mendoza G, Hinson JW, Mattsson KI, Strassle BW, Trimmer JS, Rhodes KJ (2000) Modulation of A-type potassium channels by a family of calcium sensors. Nature 403:553–556.

Cai X, Liang CW, Muralidharan S, Kao JP, Tang CM, Thompson SM (2004) Unique roles of SK and Kv4.2 potassium channels in dendritic integration. Neuron 44:351–364.

Chandy KG (1991) Simplified gene nomenclature. Nature 352:26.

Csiffary A, Gorcs TJ, Palkovits M (1990) Neuropeptide Y innervation of ACTH-immunoreactive neurons in the arcuate nucleus of rats: a correlated light and electron microscopic double immunolabeling study. Brain Res 506:215–222.

Debanne D, Guerineau NC, Gahwiler BH, Thompson SM (1997) Action-potential propagation gated by an axonal I_A-like K^+ conductance in hippocampus. Nature 389:286–289.

Fremeau Jr RT, Troyer MD, Pahner I, Nygaard GO, Tran CH, Reimer RJ, Bellocchio EE, Fortin D, Storm-Mathisen J, Edwards RH (2001) The expression of vesicular glutamate transporters defines two classes of excitatory synapse. Neuron 31:247–260.

Frick A, Magee J, Johnston D (2004) LTP is accompanied by an enhanced local excitability of pyramidal neuron dendrites. Nat Neurosci 7:126–135.

Gutman GA, Chandy KG, Adelman JP, Aiyar J, Bayliss DA, Clapham DE, Covarriubias M, Desir GV, Furuichi K, Ganetzky B, Garcia ML, Grissmer S, Jan LY, Karschin A, Kim D, Kuperschmidt S, Kurachi Y, Lazdunski M, Lesage F, Lester HA, et al. (2003) International union of pharmacology. XLI. Compendium of voltage-gated ion channels: potassium channels. Pharmacol Rev 55:583–586.

Hamori J, Szentagothai J (1980) Lack of evidence of synaptic contacts by climbing fibre collaterals to basket and stellate cells in developing rat cerebellar cortex. Brain Res 186:454–457.

Hille B (2001) Ionic channels of excitable membranes. Sunderland, MA: Sinauer.

Hoffman DA, Magee JC, Colbert CM, Johnston D (1997) K^+ channel regulation of signal propagation in dendrites of hippocampal pyramidal neurons. Nature 387:869–875.

Holderith NB, Shigemoto R, Nusser Z (2003) Cell type-dependent expression of HCN1 in the main olfactory bulb. Eur J Neurosci 18:344–354.

Hsu YH, Huang HY, Tsaur ML (2003) Contrasting expression of Kv4.3, an A-type K^+ channel, in migrating Purkinje cells and other post-migratory cerebellar neurons. Eur J Neurosci 18:601–612.

Jinno S, Jeromin A, Kosaka T (2005) Postsynaptic and extrasynaptic localization of Kv4.2 channels in the mouse hippocampal region, with special reference to targeted clustering at GABAergic synapses. Neuroscience 134:483–494.

Johnston D, Hoffman DA, Colbert CM, Magee JC (1999) Regulation of back-propagating action potentials in hippocampal neurons. Curr Opin Neurobiol 9:288–292.

Johnston D, Christie BR, Frick A, Gray R, Hoffman DA, Schexnayder LK, Watanabe S, Yuan LL (2003) Active dendrites, potassium channels and synaptic plasticity. Philos Trans R Soc Lond B Biol Sci 358:667–674.

Kosaka T, Kosaka K (2003) Neuronal gap junctions in the rat main olfactory bulb, with special reference to intraglomerular gap junctions. Neurosci Res 45:189–209.

Lorincz A, Notomi T, Tamas G, Shigemoto R, Nusser Z (2002) Polarized and compartment-dependent distribution of HCN1 in pyramidal cell dendrites. Nat Neurosci 5:1185–1193.

Maletic-Savatic M, Lenn NJ, Trimmer JS (1995) Differential spatiotemporal expression of K^+ channel polypeptides in rat hippocampal neurons developing *in situ* and *in vitro*. J Neurosci 15:3840–3851.

Migliore M, Shepherd GM (2002) Emerging rules for the distribution of active dendritic conductances. Nat Rev Neurosci 3:362–370.

Muennich EA, Fyffe RE (2004) Focal aggregation of voltage-gated, Kv2.1 subunit-containing, potassium channels at synaptic sites in rat spinal motoneurones. J Physiol (Lond) 554:673–685.

Nusser Z, Mulvihill E, Streit P, Somogyi P (1994) Subsynaptic segregation of metabotropic and ionotropic glutamate receptors as revealed by immunogold localization. Neuroscience 61:421–427.

Nusser Z, Lujan R, Laube G, Roberts JDB, Molnar E, Somogyi P (1998) Cell type and pathway dependence of synaptic AMPA receptor number and variability in the hippocampus. Neuron 21:545–559.

Palay SL, Chan-Palay V (1974) Cerebellar cortex: cytology and organization. Berlin: Springer.

Rhodes KJ, Carroll KI, Sung MA, Doliveira LC, Monaghan MM, Burke SL, Strassle BW, Buchwalder L, Menegola M, Cao J, An WF, Trimmer JS (2004) KChIPs and Kv4 alpha subunits as integral components of A-type potassium channels in mammalian brain. J Neurosci 24:7903–7915.

Schoppa NE, Westbrook GL (2002) AMPA autoreceptors drive correlated spiking in olfactory bulb glomeruli. Nat Neurosci 5:1194–1202.

Shigemoto R, Mizuno N (2000) Metabotropic glutamate receptors-immunocytochemical and in situ hybridization analyses. In: Handbook of chemical neuroanatomy (Otterse OP, Storm-Mathisen J, eds), pp 63–98. Amsterdam: Elsevier.

Trimmer JS, Rhodes KJ (2004) Localization of voltage-gated ion channels in mammalian brain. Annu Rev Physiol 66:477–519.

Varga AW, Anderson AE, Adams JP, Vogel H, Sweatt JD (2000) Input-specific immunolocalization of differentially phosphorylated Kv4.2 in the mouse brain. Learn Mem 7:321–332.